Surface analysis of corroded silver coins from the wreck of the *San Pedro De Alcantara* (1786)

I.D. MacLeod [a], E. Schindelholz [b1]

[a]Western Australian Museum, Cliff Street, Fremantle, Western Australia 6160, Australia
[b] Mariners' Museum, 100 Museum Drive, Newport News, Virginia 23606-3759

Abstract

A detailed morphological study of the corroded surfaces of seven silver "Pieces of Eight" recovered from the *San Pedro de Alcantara* shipwreck site was conducted using low pressure scanning electron microscopy (SEM) with energy dispersive spectroscopy (EDS) analysis. Mosaics of the backscattered images of the coin faces indicated that the coins consist of a solid solution of β-phase grains with α-phase inclusion and that bromian chlorargyrite is the main corrosion product. Thin surface films of hydrated iron oxides facilitated the formation of sulphide minerals on buried coins. Surfaces were heavily abraded by the harsh erosion corrosion conditions and most bear evidence of damage from impact of other artefacts on-site. Correlations exist between the surface analyses and the data from the *in-situ* corrosion measurements.

Keywords: SEM mosaics, bromian chlorargyrite, silver coins, corrosion, shipwrecks, conservation

1. Introduction

The *San Pedro de Alcantara* was a 64 gun Spanish man-of-war ship that was built in Cuba in 1770. The vessel left Peru in 1784 carrying cargo which included 420 passengers, hundreds of tons of copper and gold and more than one hundred tons of *pieces of eight* minted in Lima. Lengthy repairs in Rio de Janeiro saw the journey delayed until 1786 when the vessel sank after colliding with a rock off the coast of Portugal. One hundred and twenty-eight people, including several Peruvian prisoners, perished in the accident (Blot & Pinheiro-Blot, 1991). Given that the cargo represented 8% of Spain's total circulating currency King Charles (Carolus) III launched a salvage operation that employed 40 full-time divers for three years to recover the cargo (Blot, 2004). The diving operation was at that time the largest ever in European history and was successful in recovering the majority of the ship's cargo. The wreck site was essentially undisturbed until January 1963 when a German-built Portuguese steamship *João Diogo* ran aground less than 30 metres from the impact site of the *San Pedro de Alcantara* (Blot & Pinheiro-Blot, 1991). Salvagers blasted the hulk, which scattered the iron ore cargo and elements of the steel ship over the Spanish shipwreck site (Blot & Pinheiro-Blot, 1992).

The current site is scattered over 200 metres long in water 3-9 metres deep, lying off a rocky coast near Peniche, Portugal. The sea bottom consists of irregular rocks, with numerous cavities and crevices filled with up to 0.5 metres of stone and sand. The artefacts are mostly small objects randomly spread over the large area and located in these cavities and crevices (Blot, 1998a). The site is characterised by very high energy with waves breaking over it. Recent excavation recovered fragments of pottery, encrusted iron objects, pieces of lead sheathing, silver and gold coins, a copper ingot, and mercury deposits, and a swivel gun from the forecastle of the ship. Lead bars and iron tools related to the 18th century salvage operation were also recovered (Blot, 1998b). The maritime archaeologists developed mathematical models based on artefact distribution and the physical characteristics of the artefacts to gain insight on parameters affecting the site formation processes (Blot and Pinheiro-Blot, 1992; Blot, 1998a). The initial *in-situ* corrosion studies of silver coins focused on seven coins that represented varied geographic locations, which were subsequently recovered and these objects formed the locus of this study.

The pieces of eight (8 reales) were minted in Lima, Peru, and showed a "bust type" portrait of Carolus III on the obverse and the Spanish coat-of-arms on the reverse (Figure 1). They were minted between 1772 to 1788 when the King was succeeded by his son Carolus IV. The coins had mint dates of 1780 (no 4030), 1784 (no 4324) and 1782 for numbers 4327, 4331 and 4342 while 4315 and 4325 were too heavily abraded and could not be dated. These coins were minted on a screw press, which was operated by rotating a weighted lever that pressed an upper and lower die together with a milled or finished planchet between them (Craig *et al*., 2002). Under the intense and even pressure of the press the minters were able to produce coins with great accuracy. Their mass was 27.064 grams and the fineness of 0.90278 equated to 90.278% silver and 9.722% copper, the

[1] Corresponding author: TEL:+1 757 5917787: FAX +1 757 591 7312 e-mail: eschindelholz@mariner.org

diameter was 3.8 cm and they were 2 mm thick (Cordua, 2003). The coin weight is almost (0.955) one avoirdupois ounce.

The degree of preservation of the recovered coins related to their location on the wrecksite. Coins 4324, 4325, 4327 and 4331, which were found buried under 15cm of coarse sediment, have more or less retained their original dimensions. Coins 4315, 4030, and 4342, which were found lying atop the seabed, have lost a majority of their original surface and dimensions. There was only one coin (no.4325) with any significant amount of concretion; the deposits consisted of sand-sized to pebble-sized sedimentary particles and small shells bound together by calcareous concretion (see Figure 2). Coins 4325, 4331, 4324, and 4327 all have considerable amounts of iron corrosion products on their surfaces. Since these coins represent valuable components of Peruvian, Spanish and Portuguese cultural heritage, a non-invasive methodology of surface analysis was chosen.

Figure 1: Carolus III 1780 “bust type” piece of eight, from www.newworldtreasures.com.

A distinct and uniform mineral stratum was identified on a few coins, which may indicate physical or chemical changes in the site environment or their microenvironments over time (Robbiola *et al*, 1988). Scott (1994) has demonstrated the relationship between the composition of the corroded surfaces and the underlying original microstructures of bronze artefacts from an ancient terrestrial archaeological site and how the changes in the burial and in post-burial environments were expressed in the corroded surfaces. The authors have found related shipwreck phenomena (MacLeod, 1982; 1985; 1991; 2002) that connect the corrosion characteristics of metals with electrochemical site parameters and their metallurgical structure. Oxely (1990) stated the importance of understanding site formation processes of underwater sites with respect to artefact preservation. The same methodology was recently applied by Craig *et al.* (2002) to an 1800 Ecuadorian Spanish Piece of Eight from the wreck of the *Santa Leocadia*. Corrosion studies on marine metals have been reported by Robinson (1982), Macleod *et al.* (1986) and North and Macleod (1987) while Fox (1994) examined land corrosion.

Figure 2: Obverse surface of coin no 4325 on the left and reverse on the right.

2. Experimental Procedure

The coin surfaces were examined using reflected light microscopy and geological scanning electron microscopy (GeoSEM) in low-vacuum backscattered mode (Robinson, 1992). Backscattered image mosaics of the coin faces presented a unique view of the corrosion patterns. The primary aim of this non-destructive characterisation of the microstructure and corrosion of silver coins was to test a hypothesis on the deterioration mechanisms they underwent in the marine archaeological environment. The initial study revealed important information relating to the deterioration of the coins in the archaeological environment. Stress corrosion cracking in the form of fine fissures in the metal surface was apparent at many of the leading edges of the coins, where the raised edges are adjacent to the milled edge where distortion during striking would be at a maximum. There were numerous examples of sites where selective corrosion of the copper rich phases of the alloy had been attacked in a series of parallel lines. These were associated with stress placed on the silver during rolling of the blanks before they were cut to size. Corroded β-phase silver grains (solid solution of copper in silver) were identified on an eroded area of one coin. Redeposition of silver from a layer of corrosion products was found on the surfaces of another coin, a phenomenon that has been observed on silver coins recovered from Australian wrecks (MacLeod, 1991). Mercury and lead corrosion products, in the form of minute particles and spots, were found on the surfaces of some coins. This indicates that the coins and the original lead particles and liquid mercury existed in the same microenvironment on the wrecksite.

Each coin and their corrosion patterns were recorded with high resolution (5 mega-pixel) photographs. Images were taken of both sides of each coin using a Nikon Coolpix 5700 camera. The coins were also examined using a reflected light stereomicroscope at up to 80x magnification to provide supplementary information to the SEM/EDS analysis. Initial analyses in Australia were conducted using a Phillips XL40 scanning electron microscope with light element energy dispersive analytical x-ray detection (EDAX) and GeoSEM with low-vacuum capabilities. Although the instrument is able to work at higher pressures, stray x-ray radiation occurs when the electrons from the primary electron beam deflect off air molecules in the sample chamber and hit the specimen at considerable distances from the position of the beam (Robinson, 1992). The impact of the stray x-rays on the EDAX was minimised using a combination of between 0.2-0.8 mbar chamber pressures and a working distance of around 10 mm. The SEM was used in backscattered imaging mode to investigate the morphological and relative compositional nature of the coin surfaces. EDAX was employed to identify the elemental composition of areas of interest on the backscattered image.

Backscattered electron (BSE) photo mosaics of the coin faces were created using a software program developed by Michael Verall of CSIRO for use with the Philips XL 40. Since the typical magnifications of the BSE images of the coin surfaces cover an area of 0.04 mm^2 it was useful to have a method for gaining a composite image, since the average coin surface comprises roughly 200-300 such images. Part of the project was to see if there was any correlation between localised compositional differences and the gross features of the corroded and eroded surfaces. The software automates the SEM to capture 330 images in a string of 200x BSE pictures of the sample along a regular grid coordinate system. Although some distortion occurred around the edges of each individual image in the mosaic, the digital images of the coin faces were superimposed on the corresponding SEM mosaics using Adobe Photoshop 7.0. Using the mosaic maps with the highlighted areas of interest, a second set of SEM/EDS sessions were carried out using a Hitachi S3200 variable-pressure SEM with a Robinson backscatter detector and a light element x-ray energy dispersive spectrometer (XEDS) at the Canada Centre for Mineral and Energy Technology (CANMET) in Ottawa, Canada. The chamber pressure on the Hitachi was set to around 0.1 mbar with a working distance of 16mm.

X-ray diffraction**.** Unless otherwise stated all mineral phases were identified by x-ray diffraction. Typical 0.5 mg samples of corrosion products from coins 4342 and 4325 were placed on a zero background sample plate and run on a Phillip's Xpert MPD at 45 kilovolts and 40 milliamps for approximately one hour. The silver sulphide from the obverse of coin 4325 was adhered to the tip of a glass fiber with silicone oil and placed in Gandolfi camera and run in a helium atmosphere for 22 hours at 40 kilovolts and 22 milliamps on a Philips 2W 1010/90 generator with a cobalt source.

3. Results and discussion of the corrosion mineralogy

Calcium carbonate was abundant on every coin surface either as biogenic deposits or as inorganic crystals of magnesian calcite, ($Ca_{1-x}Mg_xCO_3$) while the polymorph magnesian aragonite was found covering large areas of coin 4327. The aragonite is in a steep pyramidal form as clusters of sharp spiked crystals (see Figure 3) The presence of this form of aragonite on coin 4327 indicates that this coin was subjected to a different microenvironment. In normal seawater of salinity 34.33% the ionic product of calcium and carbonate ions at pH 8.2 is 270 x 10^{-8}, which is much higher than the solubility product of 50 x 10^{-8} for calcium carbonate, confirms that seawater is supersaturated with respect to calcium carbonate (Horne, 1969). Any change in temperature,

salinity or pH will cause the precipitation of some form of $CaCO_3$ since the ratio of $[CO_3^{2-}]/[HCO_3^-]$ is given by the relationship,

$$log\{[CO_3^{2-}]/[HCO_3^-]\} = pH - 10.2,$$

where 10.2 is the pKa_2 of carbonic acid. In normal seawater bicarbonate is the dominant ion so any increase in the local pH will dramatically alter the activity of the carbonate ion and lead to precipitation on the coin surfaces at cathodic sites. In aerobic seawater the cathodic reduction of oxygen,

$$O_2 + 2H_2O + 4\ e^- \rightarrow 4\ OH^-$$

will cause the pH to increase on the surfaces associated with the reduction side of the corrosion process (Weier, 1971, North & MacLeod, 1987).

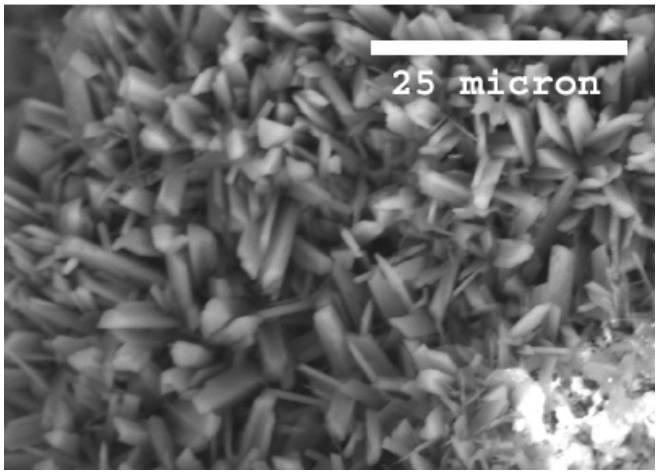

Figure 3:Field of magnesian aragonite on surface of coin no. 4327, full width 68 μm

Magnesium carbonate is much more soluble than its calcium analogue and its concentration will not normally be sufficient to allow it to precipitate. Calcareous concretions on artefacts from Australian waters are composed of a range of magnesian calcites, where 0.966 <x> 0.839 in the general formula $Ca_{(1-x)}Mg_xCO_3$ (MacLeod, 1991). The magnesium content of the calcareous deposits on the coins from the *San Pedro De Alcantara* fell in this range, with the aragonite on coin 4327 having higher levels of magnesium than the calcite on other coins. Carlson (1983) found that aragonite is the preferred mineral when higher concentrations of magnesium are present. Tribble (1993) noted that sedimentary environments rich in iron would favour aragonite formation relative to iron-deficient systems.

Milliman and Manheim (1968) reported aragonite to be the major calcium carbonate mineral in an aerobically formed concretion on an iron nail recovered from a shipwreck off the coast of Turkey. Under anaerobic conditions, when a coin is buried in the sand, or when there is a coherent layer of iron oxy-hydroxides preventing direct access of the dissolved oxygen to the corroding surface, sulphide ions from sulphate reducing bacteria are precipitated as silver sulphide (Ag_2S). The presence of iron oxides on coin 4327 provides a good rationale for the large amounts of silver sulphide present on the surfaces, and the preferential growth of aragonite on this coin. The absence of aragonite on coin 4325, which also exhibits major iron oxide and silver sulphide deposits is simply a reflection of an alternative cathodic reduction process that does not produce hydroxide ions.

The large amounts of iron found in the concretions and as distinct films on the coins recovered from a buried microenvironment is consistent with the history of the site. The majority of the surfaces of coins 4325, 4327, and 4331 were covered with a layer of pure hydrated iron oxides, such as $FeOOH.xH_2O$. The films are compact and of relatively uniform thickness. The deposition of this material is likely to have occurred during the salvaging of the *João Diogo* as a continuous film that was subsequently eroded/corroded away in areas to reveal underlying layers of silver halides. The absence of iron on coins 4315, 4030 and 4342 is a reflection that these coins are highly eroded and corroded and have very little concretion.

Redeposited silver is present on coins 4324, 4342, and 4325 as crystals that have grown on top of the crystalline primary corrosion products and on top of amorphous deposits. The exposed silver sulphide stratum underneath the iron film on coin 4325 exhibits numerous inclusions of redeposited silver crystals averaging 15 microns in length (see Figure 4). Redeposited silver crystals are commonly found underneath iron oxide films on silver coins from marine shipwrecks in Australia (MacLeod, 1991). The formation of silver crystals can be due to the poor electrical and ionic conduction properties of iron oxide films, which can limit oxygen access to the corroding metal surface and favours alternative reduction reactions such as

$$AgCl + Cu \rightarrow CuCl + Ag\downarrow$$

At chloride ion activity of 0.32 M, the cell potential for the above reaction would be around 94 mV (MacLeod, 1981). The formation of redeposited silver on coin 4324, which has a small amount of iron oxide film covering its surface, and 4342, which lacks a film, can be attributed to a different process. On these coins the redeposited silver is in the form of 5-10 micron amorphous inclusions in Ag(Cl,Br) pavements. The inclusions were only found in the smooth abraded areas of the pavements, which may be due to the fact that, during BSE examination, the abraded surfaces provided areas of higher visibility for the bright silver inclusions compared to the surrounding rough, non-abraded pavement. Both coins also contained a large amount of mercury, usually in a silver amalgam.

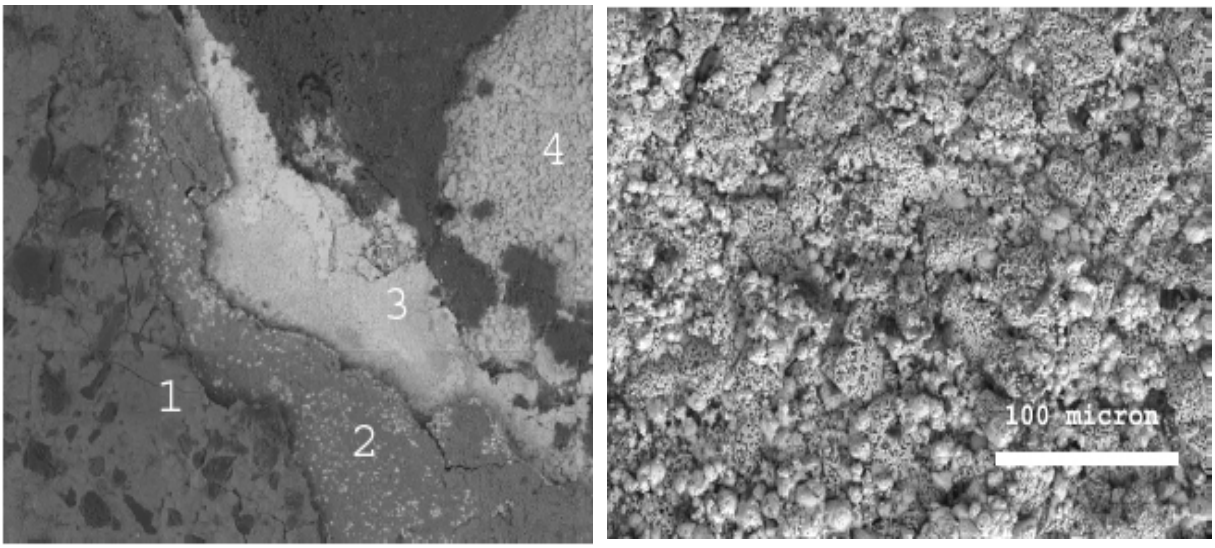

Figure 4: Left SEM photomosaic of coin 4325 showing layer 1: (lower left) hydrated iron oxides with silica inclusions, layer 2: mixed silver and copper halides, layer 3: silver sulphides, layer 4: silver halides overlaying the dark grey $CaCO_3$ deposits (image width 1100 μm). The right SEM image shows corroded redeposited silver intermixed with silver halides, width 800 μm,

The presence of mercury on these coins is not surprising given the archaeologists found a few hundred grams of mercury in the hollow of a rock on the *San Pedro de Alcantara* site, which they attributed to the mercury samples the ship was transporting when it sank (Blot & Pinheiro-Blot, 1991). The smallest amalgam deposits on coins 4324 and 4342 were discovered on the abraded areas of the Ag(Cl,Br) pavements and are identical in shape and size to the redeposited silver on these coins. From these findings, it can be hypothesized that the formation of redeposited silver inclusions involved the reduction of silver corrosion products by mercury. When mercury came in contact with the silver halides it reduced the silver and formed soluble mercuric halides. One such reaction that may have occurred is as follows:

$$2\ AgCl + Hg \rightarrow 2Ag + HgCl_2$$

The standard potential for this reaction is 62 mV, which is sufficient to allow the reaction to proceed. Mercuric chloride ($HgCl_2$) is highly soluble in seawater and would have been diffused from the reaction site. Excess mercury may have then amalgamated with the reduced secondary (redeposited) silver and the exposed underlying primary core silver, which would account for the silver amalgam inclusions as shown in Figure 5. Coins 4342 and 4324 exhibit spheres of silver amalgam between 300-500 microns in diameter resting on top of Ag(Cl,Br) pavements The ratio of mercury to silver in these alloys was determined to be 1:1 using EDS analysis. It is possible that the mercury had volatilized after excavation and during SEM examination, but it can be understood that these deposits contained at least 50% mercury at the time of their recovery. The spheres were also found to be quite porous and some have silicon inclusions. The formation process for the amalgam spheres would have been the same as that for the small amalgam inclusions discussed above.

The spherical shape of these deposits is attributed to the high surface tension of mercury and alludes to drops of mercury sitting on the surface of the coins and amalgamating the underlying primary silver. Relatively large non-spherical deposits of 1:1 amalgam are present on coins 4342, 4315, and 4030. The edges of the amalgam deposits on all of these coins are rounded hinting at the influence of surface tension on their formation. The obverse of 4030 is covered with a discontinuous layer of amalgam that contains large amounts of silicon inclusions. This coin may have at one time been sitting in a pool of mercury on the site. In addition to the amalgam on these coins, an anomalous non-spherical deposit of virtually pure mercury sits on top of an

Ag(Cl,Br) matrix on the obverse of coin 4342 The failure of the amalgam formation is likely to be due to the deposition of a siliceous organism on the coin surface which acts as an insulator.

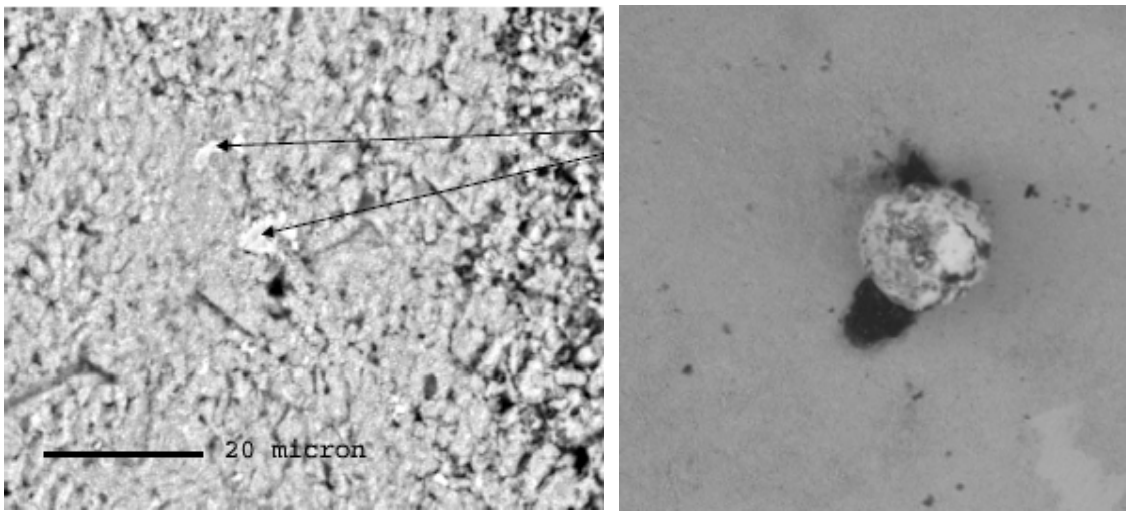

Figure 5: The left image shows the BSE images of obverse of coin no 4342, of silver amalgam (arrowed) in a silver halide matrix (image width 70 μm), right BSE image showing an amalgam sphere on coin 4342, approximate diameter 110 μm.

The major silver corrosion product found on every coin in this study is embolite Ag(Cl,Br), otherwise known as bromian chlorargyrite, with minor amounts of chlorargyrite (AgCl). The presence of these minerals is to be expected given the coins are from a shallow and energetic ocean site. Bromian chlorargyrite has been found in quantity on archaeological silver artefacts from both terrestrial and underwater environments. Since the silver ion concentration needed to precipitate AgCl from seawater is $2.92x10^{-10}$ and for AgBr it is $5.04x10^{-10}$ the coprecipitation of both halides is not unexpected. Kolthoff and Yutzy, Hedges (1976) speculated that the ratio of bromide to chloride in silver halide corrosion products from a marine environment would be on the order of 0.33 on a molar basis and analysis of a Spanish piece of eight found a similar ratio. Coins from the *San Pedro De Alcantara* site had molar ratios of bromine to chlorine in chlorargyrite from 0 to 1.0 on a molar basis, with the mode ratio being 1.0. There are two distinct phases of bromian chlorargyrite on all of the coins: amorphous particles that occur as pavements and larger isometric crystals. Except for the heavily eroded coins (4315, 4030, 4342), the coins display pavements of amorphous particles overlying a stratum of large Ag(Cl,Br) crystals measuring up to 50 microns. The large crystals are lamellar in structure and appear to be the product of recrystallisation (see Figure 6). EDS analysis of the two phases revealed no difference of Cl:Br ratios between them. Cubic crystals of chlorargyrite are present on the coins in limited quantity and were usually found intermixed with the amorphous Ag(Cl,Br) pavements. Bromargyrite (AgBr) was not observed on any of the coins in this study.

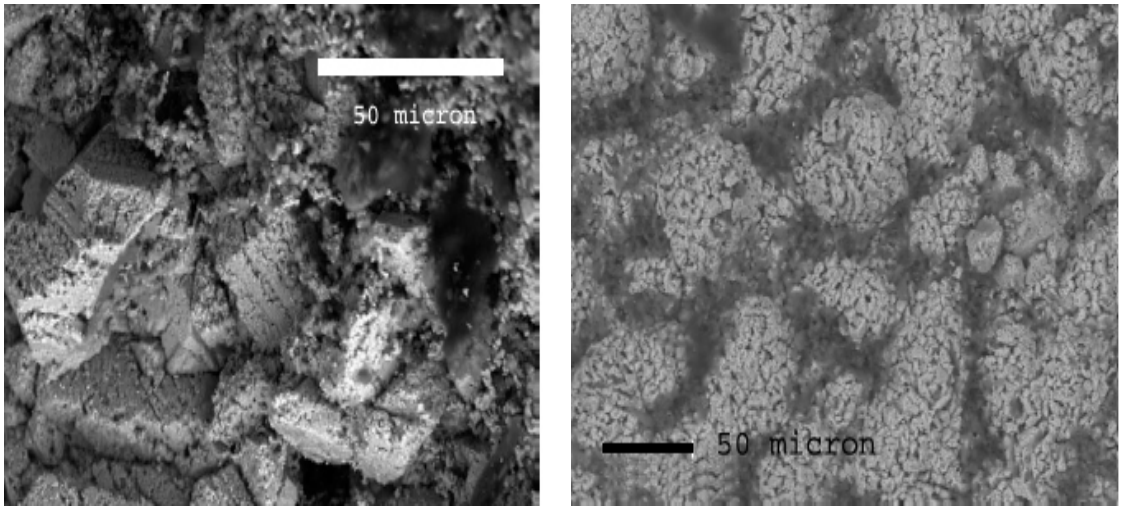

Figure 6: Left BSE micrograph of coin 4331 showing lamellar structure of large Ag(Cl,Br) crystals, image width 140 μm and the right image from the reverse of coin 4325 showing crystals in the process of recrystallising, image width 300 μm

Deposits of silver sulphide (Ag_2S) are present on coins 4325 and 4327 as distinct layers (that also contain small amounts of copper) were found under hydrated iron oxide films. The silver sulphide layer (see layer 2 from the left image in Figure.4) on the obverse of coin 4325 consisted of monoclinic acanthite (Ag_2S) and the presence of some argentite. This body-centered cubic polymorph of acanthite, is indicated by the presence of very similar lines, since the 2θ angles for argentite are very close to certain angles in the acanthite pattern. Both Ag_2S forms have been found on silver-copper alloys artefacts from shipwreck sites in Australia (North and MacLeod, 1987) with acanthite the dominant sulphide corrosion products on coins from the *Rapid* shipwreck (MacLeod, 1991). Given that no other reports of naturally occurring argentite have been encountered in the biosphere, it is likely that the inherently unstable argentite could be explained by the stabilization of argentite by copper atoms (McNeil and Little, 1992) Argentite, but not acanthite, can accommodate up to approximately 30% copper in its lattice structure which could make it more stable on a silver-copper alloy coin (McNeil and Little, 1999). This could explain the presence of copper in the silver sulphide layer on coin 4325 and the lack of copper sulphides or silver copper sulphides in the XRD analysis results. The large number of silver-copper-sulphide corrosion products on shipwreck artefacts is due to the ubiquitous presence of sulphide ions resulting from the metabolic activity of sulphate reducing bacteria as noted by Craig *et al.* (2002). The presence of silver sulphide layers underneath iron corrosion products on coins 4325 and 4327 is consistent with an anaerobic microenvironment under the iron while the coins were in an aerobic environment (McNeil and Little, 1999). Alternating cycles of burial and exposure can also explain the presence of Ag(Cl,Br) layers underneath the silver sulphide layers on both coins.

Apart from possible copper sulphides on coins 4325 and 4327, aerobic copper corrosion products cover large areas of the surface of every coin in this study. Generally the minerals exist as small and numerous deposits intermixed with the Ag(Cl,Br) matrices or as large overlying deposits on the surface of the coins. XRD and EDS analysis show the compounds consist of a variety of copper (II) chloride compounds and copper oxides, including clinoatacamite, $Cu_2Cl(OH)_3$. The greater mobility of copper chloride complexes such as $CuCl_2^-$ accounts for the overlying copper corrosion deposits on the coins. Raised islands of copper corrosion products overlying the silver halide surfaces are present on the heavily deteriorated coins. The greater Mohs' hardness of copper oxides and chlorides (3 hardness) compared with silver halides (1.5-2 hardness), would leave islands of copper corrosion products in an erosion situation that reflects the extremely turbulent nature of the *San Pedro De Alcantara* wrecksite.

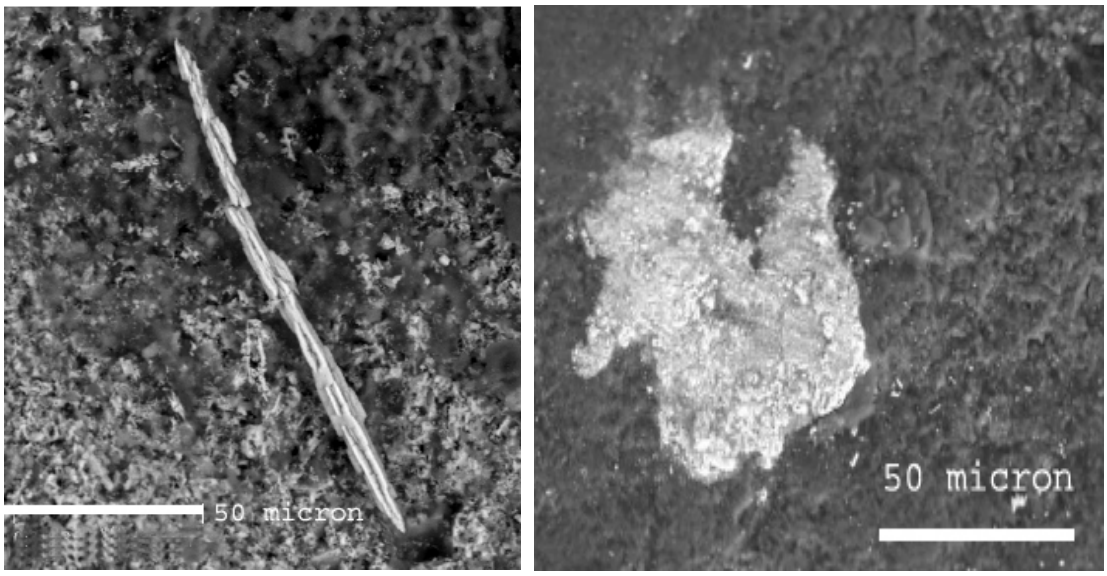

Figure 7: Left BSE image of the reverse surface of coin no 4030 showing an anglesite crystal, image width 140μm and on the right, an image from the obverse of the same coin on the obverse showing laurionite in a calcium carbonate matrix, width of 110 μm

Many anglesite ($PbSO_4$) crystals were found on the surface of coin 4030 along with deposits of laurionite (PbClOH) in the iron-bearing calcium carbonate concretions. Anglesite crystals covering the enormous range of 2-200 μm in length were found on both faces of the coin and have a tabular bladed appearance dominated by large pinacoid faces (see Figure 7). Most of the anglesite was found sitting on top of or intermixed with loose sand debris and calcite crystals in the niches of calcareous concretions. Laurionite was found as discrete amorphous deposits in the iron-bearing calcareous concretions on the obverse of this coin, mainly on the concretion edges. Coin 4030 is the only coin of the seven that bears lead minerals. Although it was not found near any lead artefacts, it could be postulated that the coin was at one time in close association with lead since both minerals are highly insoluble in seawater. Large crystals of calcium sulphate ($CaSO_4$) present on coins 4324, 4327, and 4331 are a likely consequence of iron corrosion products acting as ion exchange sites, which regularly concentrates sulphate ions so that the normally soluble minerals would precipitate on the coin surfaces.

3.2 Erosion Corrosion

Erosion corrosion is indicated by an increased rate of deterioration on a metal because of the relative movement between a corrosive fluid and a metal surface (Shrier, 1976). Since the *San Pedro de Alcantara* site is an area of constant and aggressive surge action, erosion corrosion plays a major role in the deterioration of metals on this site. The coins 4342, 4030 and 4315 were found lying on top of the sediment and their much higher mass loss is a measure of the erosion effect. Prior to recovery, coin 4315 was lying flat on top of a thin layer of sediment in a shallow bedrock hole, which meant it was fully exposed to water and sediment movement, and this resulted in more than a 60% mass loss. The majority of the coin is covered with a thin pavement of amorphous Ag(Cl,Br) with inclusions of copper corrosion products but in some areas the core metal of the coin is actually exposed since the erosion was so severe as to prevent precipitation of corrosion products. There are a few small remnants of raised calcareous concretions on the coin that are resting on eroded and corroded silver halide pedestals, the shape of which indicates that they were being eroded and corroded away in preference to the concretions, since calcite and aragonite have Mohs' hardness of 3 compared with 1.5-2 for bromian chlorargyrite. Two other heavily deteriorated coins, 4342 and 4030, display a similar concretion pattern.

Although hardness is a fairly good criterion for resistance to mechanical erosion or abrasion, it does not necessarily succeed as a good criterion for predicting resistance to erosion corrosion. The ability of a surface film or layer to passivate the underlying metal is also an important factor. Calcareous concretions, especially those that grow in tropical waters tend to be somewhat porous and good conductors for the corroding metal they cover (MacLeod, 1982). In contrast, iron oxide films tend to be poor ionic and electrical conductors and can passivate the underlying corroding metal. There is a clear discrepancy between the preservation of those coin surfaces that are covered by iron oxide films and those that are not. Where the surface of coins 4325 is covered by an iron oxide film the raised design is well preserved, while the surfaces without the protective iron have the design obliterated. Clearly the iron oxide films are providing erosion and corrosion resistance to the coin surfaces they cover. It appears that the combination of the hardness of the marine iron oxides, from 4.5 to 6 on the Moh's scale, and their low conductivity accounts for the protection against erosion corrosion.

An unusual erosion corrosion phenomenon is found on many of the coins where the iron oxide films or thin calcareous concretions that were covering the raised lettering and design have worn away. In most of these areas there is only a hole that perfectly conforms to the shape of the eroded and corroded away raised design surrounded by an iron oxide film or concretion. The formation of these negative concavities most likely involved multiple steps, as indicated in Figure 8 for coin 4327, with the initial step involving the selective erosion of the topographical high points of the film or concretion.

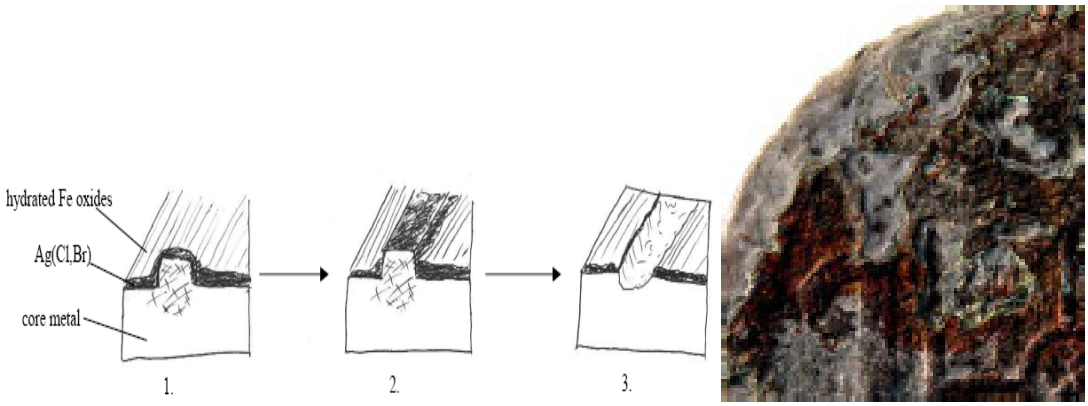

Figure 8: Erosion corrosion mechanism for preferential deterioration of raised surfaces on coin 4327.

The likely second step involved the erosion corrosion of the softer and more conductive silver corrosion products that were exposed from step one. Due to the inherent stress (hatch marks in Figure 8) in the raised areas of the coins that was caused by cold-stamping, the raised points were probably corroded in preference to their surroundings

3.3 Metallurgical Evidence

An example of stress related deterioration is seen on coin 4315, which exhibits strain lines on one edge of its obverse side (see left side of Figure 9). The strain lines, manifested by epitaxial copper (II) chloride growth in an amorphous Ag(Cl,Br) pavement, are evidence of residual stress caused during manufacture (Allen, 1969). The epitaxial growth of copper corrosion products is due to the fact that strain and slip lines can act as barriers for the migration of impurities in an alloy, causing these constituents to accumulate in those regions (Costa, 2001).

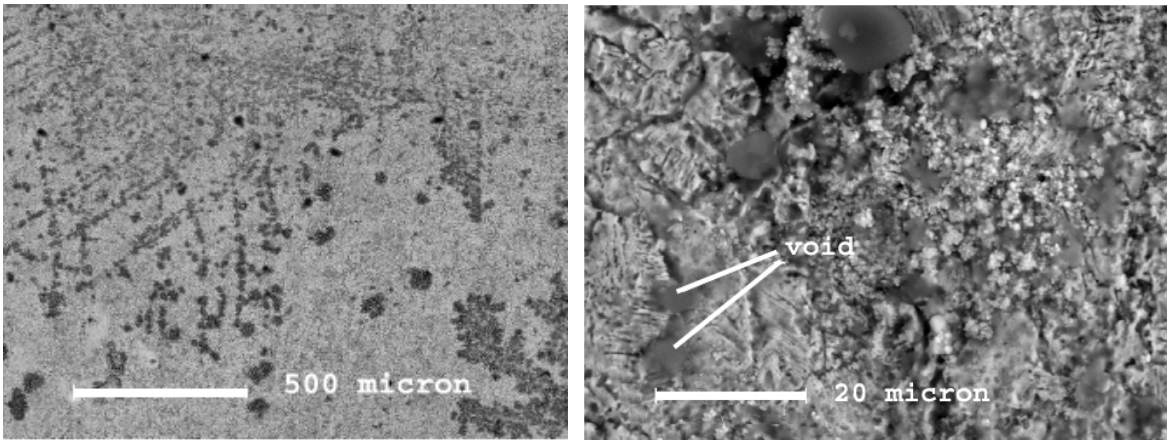

Figure 9: Left, BSE image from the obverse of coin 4315 showing Cu(II) chloride inclusions in an Ag(Cl,Br) pavement, image width 1650 μm, right image, the same surface showing exposed primary β silver grains, width of 80 μm.

The impurity in this case would be copper, given the room temperature solubility of copper in silver is only 0.1% (Butts, 1967). The precipitation of copper, usually along grain boundaries, from a solid silver-copper solution has been observed to occur on an archaeological time scale (Scott, 1991b). Additional evidence of manufacture is seen on the exposed core metal on the obverse of coin 4315, where the metallurgical grain structure is apparent, as seen in Figure 9. The microstructure of the coin was originally composed of a solid solution of β-phase grains with α-phase inclusions, which are now voids, in and surrounding the grains. This type of microstructure is characteristic of silver-copper alloys with copper contents between 5-10% *(*Costa, 2001). The absence of the α-phase (silver in copper) can be attributed to the selective corrosion of copper due to galvanic effects. Analysis of the area shown in the right hand image in Figure 9 showed it to consist of pure silver.

3.4 *In-Situ* Corrosion Potentials

The *in-situ* corrosion potentials of eleven coins, including those in this study were measured along with the pH, temperature and water depth. This data has previously been reported and it was found that there was a linear relationship between the corrosion potential (E_{corr}) and the water depth, according to the linear relationship,

$$E_{corr} = -0.273 - 0.024\, d$$

Where *d* is the water depth in metres. The square of the correlation coefficient for the nine coins described in the above equation was 0.6946, which indicates a moderate correlation between the data points and this is seen in the errors associated with the intercept value of –0.273±0.032 and the slope value is –0.024±0.006 (MacLeod, 2002a). Despite these limitations the data appears to follow the general trend observed on iron fastenings of a linear decrease in the value of E_{corr} with water depth (MacLeod, 1989). The weight of the excavated coins used

in this study and their corrosion potentials are listed in Table 1. Since all the coins had the same original weight and shape, the weight loss is a measure of the combined effects of erosion and corrosion. The data in Table 1 approximated a linear relationship between the weight loss and the corrosion potential,

$$\text{Weight loss (grams)} = 40.7 + 79\ E_{corr},$$

where the square of the correlation coefficient was 0.9222 for all but the coin 4315, which was exposed to breaking waves during heavy seas and had higher weight loss than predicted by the above equation. Despite the relatively large errors associated with the intercept (± 4.74 g) and the error in the slope (± 11.5) the data indicates that the net weight loss is linked to the corrosion potentials of the coins and thus the water depth. The apparent linear relationship between weight loss for coins and the water depth, via the E_{corr} data, indicates that different corrosion processes control the decay of the coins compared with those observed on iron shipwrecks in open waters and those in Chuuk Lagoon (MacLeod, 2002b) where there is a linear relationship between the log of the corrosion rate and water depth.

Table 1: Corrosion parameters for the silver coins

Coin reference	4315	4325	4331	4327	4342	4324	4030
Ecorr volt vs. Ag/AgCl	-0.408	-0.454	-0.452	-0.422	-0.380	-0.386	-0.374
Weight, gram	10.980	23.150	21.180	20.030	15.350	17.260	16.650

More measurements are needed before any definitive comments can be made on the relative importance of abrasion and corrosion of coins on this shipwreck site. Despite the fact that changes in microenvironment, such as coin movement and wave action, can dramatically change the corrosion potential, this preliminary study indicates that further work is likely to assist in clarifying the deterioration mechanisms.

4. Conclusion

The corrosion mineralogy and metallurgy of seven coins from the *San Pedro de Alcantara* shipwreck site in Portugal has been characterised through a combination of light and scanning electron microscopic techniques with mineral characterisation through application of quantitative x-ray analysis by EDAX and by x-ray diffraction. The physical location of the coins on the wreck site was found to be closely correlated with the specific corrosion microenvironment that was reflected in the vary degrees of corrosion, as measured by weight loss and loss of surface profile. When coins had been recovered from a similar burial environment their physical mass was similar. Aerobic environments dominate the wrecksite and this is reflected in the presence of bromian chlorargyrite, chlorargyrite, and copper (II) chlorides and oxides on the coins. Distinct layers of silver sulphide overlay bromian chlorargyrite strata on coins that were protected by the deposition of dense and electrically insulating hydrated iron-oxide films. Since the iron-oxide films are much harder than the underlying silver and copper corrosion products they provide erosion resistance. Similarly the concretions also protect the coins from erosion corrosion. The deposition of inorganic calcite is attributed to the increased pH associated with cathodic reduction of oxygen on the surfaces of the coins. Inorganic aragonite was only found on coin 4327, which is likely to be due to the large amounts of iron oxides and sulphide minerals on this coin. The site can produce such harsh erosion corrosion conditions that some surfaces were completely stripped of corrosion products. Signs of residual stress from the manufacture of the coins were apparent, which demonstrated that the coin had not been annealed after being minted. Mercury, coming from the original cargo, and its resultant silver amalgam were found on top of and sometimes intermixed with the bromian chlorargyrite pavements on the unburied coins. The discovery of large amounts of lead minerals on the surface of coin 4030 attested to its former close proximity to corroding lead objects. It was found that the weight loss of the coins could be regarded as a measure of the degradation rate and that there was a direct relationship between the corrosion potential and the weight loss of the coins.

Acknowledgements

We are deeply indebted to Bruce Robinson and Michael Verall of the Electron Beam Laboratory at the Commonwealth Scientific and Industrial Research Organization (CSIRO), Australia; and Rolando Lastra of the Canada Centre for Mineral and Energy Technology (CANMET) Mining and Mineral Science Laboratories for providing countless hours of assistance with the SEM analysis and for their insight. Special thanks to Alan Grant of Queen's University for providing his time and aid in carrying out the XRD analysis and to Alison Murray and Vera de La Cruz for their counsel. Without the inspiration of Jean-Yves Blot of the Portuguese

Institute of Archaeology, who supplied the coins from *San Pedro de Alcantara* shipwreck, this project would never have been initiated.

References

Allen, D. K., (1969) *Metallurgy Theory and Practice.* Chicago: American Technical Society.

Blot, J.-Y., Pinheiro-Blot, M.L., (1991) *Le naufrage de San Pedro de Alcantara*. La Recherche 230 Mars 22: 334-342.

Blot, J.-Y., Pinheiro-Blot, M.L., (1992) *O "interface" história-arqueologia: O caso do "San Pedro de Alcantara" 1786.* Lisbon: Academia de Marinha.

Blot, J.-Y., "San Pedro de Alcantara," http://www.abc.se/~pa/mar/spa.htm (Accessed January 25, 2004).

Blot, J.-Y., (1998a) *First steps in the analysis of ship overload*. Archaeological Computing Newsletter 51: 1-12.

Blot, J.-Y., (1998b) *From Peru to Europe (1784-1786): field and model analysis of a ship overload*. Bulletin of the Australian Institute for Maritime Archaeology 22: 21-34.

Butts, A, (ed.), (1967) *Silver: Economics, Metallurgy and Use.* Princeton, NJ: Van Nostrand.

Carlson, W.D., (1983) *The polymorphs of $CaCO_3$ and the aragonite-calcite transformation.* In Reviews in Mineralogy, vol. 11, ed. Richard J. Reeder, 191-225. Washington, D.C.: Mineralogical Society of America.

Cordua, W. S., (2003) *Pieces of eight minerals*. Leaverite news<http://www.uwrf.edu/~wc01/leaverite.html>

Costa, V., (2001) *The deterioration of silver alloys and some aspects of their conservation.* Reviews in Conservation *1.2: 18-34.*

Craig, J. R., *et al*. (2002) *Corrosion mineralogy of an 1800 Spanish piece of eight*. The Canadian Mineralogist 40: 585-594.

Fox, G. L., (1994) *Cupreous metal corrosion at a Bronze Age marine archaeological site: a study of site processes at Tel Nami, Israel*. The International Journal of Nautical Archaeology 23 (1): 41-47.

Hedges, R.E.M., (1976) *On the occurrence of bromine in corroded silver*. Studies in Conservation 21: 44-46.

Horne, R. A., (1969) *Marine Chemistry; The Structure of Water and the Chemistry of the Hydrosphere.* New York: Wiley-Interscience.

Kolthoff, I.M., Yutzy, H.C., *Studies on aging precipitates XV: the mechanism of the interaction between dissolved bromide and solid silver chloride*. Journal of the American Chemical Society 59: 2029-2032.

MacLeod, I.D., (1981) *Shipwrecks and applied electrochemistry.* Journal of Electroanalytical Chemistry 118: 291-303.

MacLeod, I.D., (1982) *The formation of marine concretions on copper and its alloys*. International Journal of Nautical Archaeology and Underwater Exploration 11: 267-275

MacLeod, I.D., (1985) *The effects of concretion on the corrosion of non-ferrous metals*. Corrosion Australasia 10 (4): 10-13.

MacLeod, I.D., (1989). *Electrochemistry and conservation of iron in sea water*, Chemistry in Australia, 56(7). 227-229.

MacLeod, I.D., (1991) *Identification of corrosion products on non-ferrous metal artefacts recovered from shipwrecks*. Studies in Conservation *36: 222-234.*

MacLeod, I.D., (2002a) *Effects of structure and composition on the performance of gold and silver alloys on shipwrecks*. Proceedings of International Congress on the Conservation and Restoration for Archaeological Objects. 178-185. Tokyo: National Research Institute for Cultural Properties.

MacLeod, I.D., (2002b) *In situ corrosion measurements and management of shipwreck sites*. In International Handbook of Underwater Archaeology, eds. Carol V. Ruppé and Janet F. Barstad, 697-714. New York: Kluwer Academic/Plenum Publishers.

MacLeod, I.D., (2003) "*Metal corrosion in Chuuk Lagoon: A survey of iron shipwrecks and aluminium aircraft,* Report to the US National Parks Authority, Pacific Division, San Francisco, USA, pp 1-92.

MacLeod, I.D., *et al. 1986. The excavation, analysis, and conservation of shipwreck sites.* In Preventive Measures During Excavation and Site Protection, *113-132. Rome: ICCROM.* McNeil, B. Michael and Brenda J. Little. (1992) *Corrosion mechanisms for copper and silver objects in near surface environments.* Journal of the American Institute for Conservation 31 (3): 355-366.
–
McNeill, & Little (1999) *The use of mineralogical data in interpretation of long-term microbiological corrosion processes: sulfiding reactions*. Journal of the American Institute for Conservation 38.2: 186-199.

Milliman, J. D., Manheim, F. T. (1968) *Submarine encrustation of a Byzantine nail*. Journal of Sedimentary Petrology 38.3: 950-953.

New World Treasures. (2003) <www.newworldtreasures.com> (Accessed April 12, 2004).

North, N. A., MacLeod I. D., (1987) *Corrosion of metals*. In Conservation of Marine Archaeological Objects, ed. Colin Pearson, 68-99. London: Butterworths.

Oxley, I., (1990) *Factors affecting the preservation of underwater archaeological sites*. International Journal of Nautical Archaeology*, 19.4: 340-341.*

Robbiola, L., et al. (1988) *Etude de la corrosion de bronzes archéologiques du Fort-Harrouard: altération externe et mécanisme d'altération stratifiée*. Studies in Conservation 33 (4): 205-215.

Robinson, B.W., (1992) *The "GeoSEM": a low-vacuum SEM optimized for geology and metallurgy*. Journal of Computer-Assisted Microscopy, 4 (3): 235-239.

Robinson, W. S., (1981) *First Aid for Marine Finds. London: The Trustees of the National Maritime Museum.*

Robinson, W. S., (1982) *The corrosion and preservation of ancient metals from marine sites*. The International Journal of Nautical Archaeology 2 (3): 221-231.

Scott, D.A., (1991a) *Metallography and Microstructure of Ancient and Historic Metals.* Santa Monica: Getty Conservation Institute.

Scott, D.A., (1991b). *A technical and analytical study of two silver plates in the collection of the J. Paul Getty Museum*. In Materials Issues in Art and Archaeology II, eds. Pamela B. Vandiver *et al.*, 665-690. 68

Scott, D.A., (1994) *An examination of the patina and corrosion morphology of some Roman bronzes*. Journal of the American Institute for Conservation 33 (1): 1-23.

Shrier, L.L., ed. (1976) *Corrosion,2nd ed., vols. 1&2., Newnes-Butterworths, London:*.

Tribble, G. W., (1993) *Organic matter oxidation and aragonite diagenesis in a coral reef.* Journal of Sedimentary Petrology 63.3: 523-527.

Weier, L.E., (1971) *The Deterioration of Inorganic Materials under the Sea.* London: University of London, Institute of Archaeology

